

The ϵ Phase of Solid Oxygen: Evidence of an O₄ Molecule Lattice

Federico A. Gorelli,^{1,3,*} Lorenzo Ulivi,^{2,†} Mario Santoro,^{1,3,‡} and Roberto Bini^{3,4,§}

¹*Dipartimento di Fisica dell'Università di Firenze and INFM, Largo E. Fermi 2, I-50125 Firenze, Italy*

²*Istituto di Elettronica Quantistica, Consiglio Nazionale delle Ricerche, and INFM Via Panciatichi 56/30, I-50127 Firenze, Italy*

³*LENS, European Laboratory for Non-linear Spectroscopy, Largo E. Fermi 2, I-50125 Firenze, Italy*

⁴*Dipartimento di Chimica dell'Università di Firenze, Via G. Capponi 9, I-50121 Firenze, Italy*

(Received 2 July 1999)

We report a detailed experimental characterization of the infrared absorption properties of the high pressure, red phase of oxygen. Spectra are measured in the far infrared, down to 100 cm⁻¹, in the fundamental vibration and in the overtone regions up to 63 GPa. A new, strong peak is observed at about 300 cm⁻¹. Samples less than 0.5 μm thick were produced to measure the strong vibron mode avoiding saturation. We find that the diatomic oxygen molecule is not a good basis to describe the vibrational spectrum of the ϵ phase. The spectra can be interpreted in a straightforward way on the basis of an association among the oxygen molecules leading to the formation of O₄ units.

PACS numbers: 62.50.+p, 63.20.Dj, 78.30.-j

Applying pressure to molecular crystals up to the Mbar range makes it possible to induce drastic changes in the intermolecular interactions. Metallization and polymerization are the two classes of phenomena, of great interest from both a chemical and a physical point of view, which are consequences of the pressure-induced transformation of the chemical bonding in the simplest molecular crystals. Metallization of simple homonuclear molecular crystals was observed first in solid iodine [1], but it was the first report on solid hydrogen which greatly stimulated the high pressure research in this direction [2]. Even though the metallization in solid hydrogen is still controversial, this phenomenon has been observed in other important model systems: in solid oxygen it was recently detected at 96 GPa [3]. Pressure-induced polymerization in unsaturated molecules occurs, due to a reconstruction of the chemical bond, usually at relatively low pressure (4–20 GPa) and it has been observed in triply bonded molecules as acetylene [4] and cyanogen [5], and in molecules possessing double bonds as carbon monoxide [6] and carbon disulfide [7].

With respect to this class of phenomena, solid oxygen represents a very peculiar case. At pressures below $\cong 10$ GPa, its phase diagram resembles closely that of other molecular crystals such as nitrogen: it is characterized by a sequence of different structures, where the molecular bond is not much altered by the increased intermolecular interaction induced by the application of pressure. At room temperature, these phases are, in order of increasing pressure, the $Pm\bar{3}n$ γ -O₂, the $R\bar{3}m$ β -O₂, and the $Fmmm$ δ -O₂ [8]. These low pressure phases, with the exception of the γ phase, are characterized by a layered structure with the oxygen molecules perpendicular to a crystal plane and parallel within the layer [9]. At low temperature, only the low pressure $C2/m$ α phase is well characterized [10], and the assignment of the region of the phase diagram above 0.4 GPa to the δ phase is un-

certain [11]. In nitrogen and other similar systems, even above $\cong 10$ GPa, the molecular unit is a good basis for the interpretation of the experimental data, and the phase changes can be explained by adjusting fine details of the intermolecular interaction. The energy difference among the various structures is small, as suggested by the large metastability domain at the phase boundaries. On the contrary, oxygen at 10 GPa transforms to a phase (ϵ or “red”) which is then stable in a vast pressure and temperature range, at least below 600 K and up to 96 GPa, which is the pressure where oxygen metallizes. The structure of ϵ phase is monoclinic $A2/m$ with $Z = 8$, but the exact positions of the molecules and the local (site) symmetry is still unknown [12,13]. The transformation to the ϵ phase is accompanied by a strong variation of thermodynamic and optical properties, namely, a big volume reduction [14], a dramatic color change [15], and the appearance of a very strong infrared absorption [16]. These characteristics lead to the conclusion that the internal energy of the ϵ phase is much lower than that of the other low pressure phases of oxygen, suggesting a qualitative change in the intermolecular interaction.

We report here the first detailed experimental characterization of the infrared absorption properties of the red phase of oxygen. The results of this study are the observation of a new strong peak (ν_{FIR}) in the far infrared region, and the direct measurement of the intensity (avoiding saturation thanks to a special loading technique) of the band (ν_{MIR}) in the O₂ fundamental vibration region. The spectra can be interpreted on the basis of an association between oxygen molecules leading to the formation of stable O₄ molecular units.

High purity oxygen was filled into a membrane diamond anvil cell (MDAC) by means of the cryogenic loading technique.

The ϵ phase was studied at room temperature in the 10–63 GPa pressure range with samples of thickness

ranging from 20 to 50 μm . To avoid saturation of the intense peak around 1500 cm^{-1} we produced samples of very small thickness ($\leq 0.5 \mu\text{m}$) by filling the gasket hole with a pellet of NaBr, removing part of it in the form of a thin slab, and then filling it with oxygen in the usual way. With these samples we performed room temperature experiments up to 24 GPa, which allowed us to measure the absorption peak of the ν_{MIR} mode without saturation.

Our standard optical setup for Fourier-transform infrared measurements with the diamond anvil cell has been described elsewhere [17]. To measure absorption in the far infrared, we had to compensate the diffraction losses due to the small dimensions of the sample, which increase drastically with the wavelength. To this aim, a new, more efficient optical condensing system was built, where the infrared beam is focused and collected by means of two ellipsoidal, aluminum-coated mirrors. These substitute the more common Cassegrain micro-objectives, with the advantage of a larger aperture and avoiding the losses due to the central aperture stop. The new setup gains about a factor 4 in the throughput, allowing the frequency range to be extended down to 100 cm^{-1} . Below 500 cm^{-1} we used a Hg vapor lamp as our source, a 6 μm mylar beam splitter, and a liquid helium cooled bolometer as a detector.

In Fig. 1, we report some of the infrared spectra collected in the ϵ phase, in the far-IR (100–700 cm^{-1}) and mid-IR region (1200–1800 cm^{-1}). Upon increasing pres-

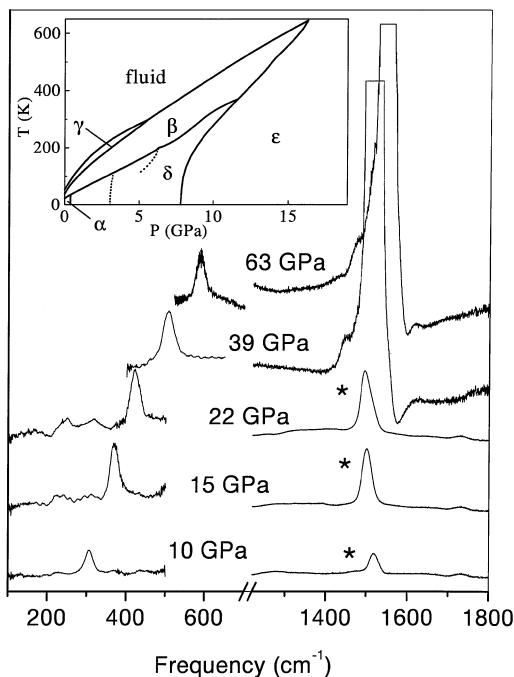


FIG. 1. Room temperature infrared absorption spectra from 100 to 1800 cm^{-1} . The spectra marked with the asterisks are obtained on samples 0.4 (± 0.1) μm thick, while the other spectra refer to samples 50 (± 1) μm thick. In the inset, the phase diagram of oxygen is reported.

sure at room temperature, the strong infrared activity appears abruptly in both regions at the δ - ϵ transition. The spectra marked with the asterisks show the 1500 cm^{-1} band without saturation. They refer to the experiments performed on the thin slab and must be multiplied by a factor ≈ 130 to be rescaled to the other spectra. This normalization factor has been estimated *a posteriori* from the intensity of the overtone bands which have been measured in all of the samples.

A surprising result is the strong absorption arising at about 300 cm^{-1} . This frequency is too high to be interpreted as a lattice mode, as can be estimated by the phonon side bands of the infrared peak measured in the stretching region at low temperature [11]. Another remarkable result is obtained from the measurements of the intensity of both infrared bands. We compare these intensities to those of infrared active modes in CO_2 and N_2O crystals, and also to the intensities of the Davydov components observed at low temperature in oxygen, below 8 GPa [11], and in nitrogen at about 20 GPa [18]. We use for this purpose the quantity $\chi = I/\rho d$ reported in Table I, where I is the measured integrated absorbance, ρ is the density, and d is the optical thickness. The latter is derived in this case from the frequency of the interference fringes observed in the single-beam spectrum. We can observe that the χ value of the ν_{MIR} mode is of the same order of magnitude as that of the stretching modes in solid CO_2 and N_2O , which are infrared allowed in the isolated molecule, and 3 and 4 orders of magnitude larger than that of the infrared Davydov component induced by crystal field in the low temperature phases of crystalline oxygen and nitrogen, respectively. The χ value of the ν_{FIR} mode, even if smaller than those of the allowed infrared modes of solid CO_2 and N_2O , is still 2 orders of magnitude larger than that of the nitrogen Davydov component.

The intensity and the frequency of the ν_{FIR} mode grow rapidly as the pressure increases. The completely

TABLE I. Normalized intensity χ of the internal modes of solid oxygen and nitrogen (infrared forbidden in the isolated molecule), and of vibrational modes of other molecular crystals (infrared allowed in the isolated molecule). The value in parenthesis is the estimated error on the last digit of χ .

Crystal	Mode	ν (cm^{-1})	χ (cm^2/g)
CO_2^{a} ($P \approx 0$)	a.s. ν_3	2343	31.40
	b. ν_2	657	5.27
$\text{N}_2\text{O}^{\text{a}}$ ($P \approx 0$)	a.s. ν_3	2235	15.85
	s.s. ν_1	1293	2.80
	b. ν_2	589	0.69
nitrogen (40 K, 19 GPa) ^b	s.s. ν_2	2370	$4.1(4) \cdot 10^{-4}$
oxygen (23 K, 7.2 GPa)	...	1549	$7.1(7) \cdot 10^{-3}$
oxygen (ϵ 20 GPa)	ν_{MIR}	1500	13(3)
	ν_{FIR}	400	0.07(2)

^aRef. [19]; ^bRef. [18].

different behavior of the frequency position of the ν_{MIR} peak, which decreases after the δ - ϵ transition, is impressive.

This process is better illustrated in Fig. 2, where the evolution of the frequencies of the two infrared bands is reported as a function of pressure. For the ν_{MIR} mode a pronounced minimum occurs at about 20 GPa, with a decrease of 40 cm^{-1} with respect to the frequency value measured immediately after the δ - ϵ phase transition. The agreement between the data collected on the thin slab, releasing pressure from 24 GPa, and those derived from the saturated absorption measured in the thicker crystal, is quite good, so that we can also confidently validate the high pressure values. The frequency of the ν_{FIR} mode presents a completely different behavior: it increases steeply up to about 20 GPa and then the slope softens regularly up to the higher investigated pressures. The frequency of the Raman mode, measured at about 1600 cm^{-1} , shows a still different evolution with pressure: it is almost constant up to 20 GPa and then it hardens linearly with a slope intermediate between the two infrared modes [20].

Contrary to the pronounced differences in the frequency behavior with the pressure of the two infrared modes, a striking similarity is found in the evolution of the intensities (see Fig. 3). The data relative to the ν_{MIR} mode are limited to 24 GPa being measured in the thin slab experiment. The intensity of both peaks increases

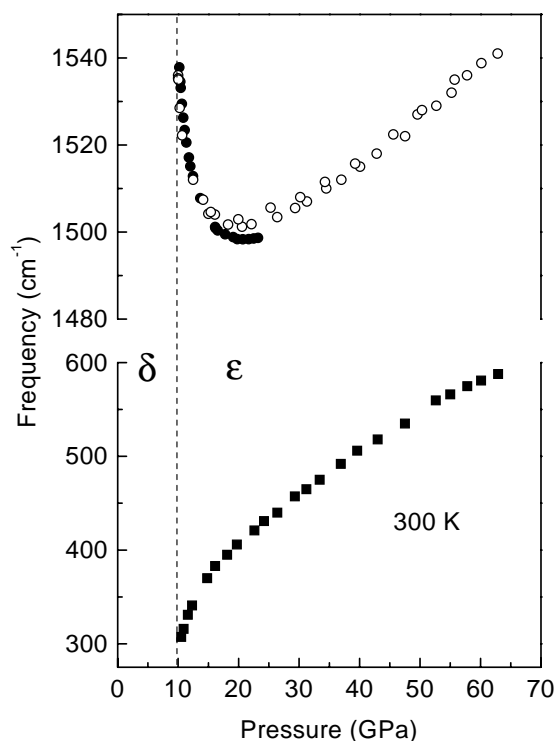


FIG. 2. Pressure behavior of the peak frequencies. The dots refer to the ν_{MIR} mode (solid dots: data collected on the thin slab; open dots: data derived from the saturated absorption peak). The solid squares refer to the ν_{FIR} mode.

very steeply up to 20 GPa, where a kind of saturation effect occurs. Therefore, at about 20 GPa, we have the coincidence of the two effects concerning, respectively, frequency and intensity evolution with pressure.

The amazing similarity between the pressure behavior of the integrated intensity of the two peaks confirms the same nature (internal vibration) of the two modes.

We can consistently interpret all of these results by assuming that between 10 and 20 GPa the charge transfer mechanism, which is already important at lower pressure [11], becomes so efficient that it leads to the formation of a chemical bonding between neighboring molecules. We can therefore analyze the spectrum on the basis of a different molecule whose process of formation is tuned by pressure and presumably extends from 10 to 20 GPa. The simplest unit we can consider derives from the bonding of two oxygen molecules. The geometry of the O_4 unit can be confidently considered rectangular, i.e., having a D_{2h} symmetry, according to the following considerations. At the δ - ϵ phase transition there is a strong volume reduction that is essentially driven by a contraction in the plane bc containing the centers of mass of the parallel oxygen molecules [14]. Between 13.7 and 35 GPa, the distances between the molecules in the bc plane reduce about 10% (being of the order of 2.5 – 2.2 \AA at 35 GPa) while the distances between the closest oxygen atoms of molecules sitting in different planes are always larger [16]. These pure geometrical considerations suggest that the new bond arises between neighboring molecules in the bc plane. A D_{2h} geometry was found to be the most stable also for $(\text{O}_2\text{-O}_2)$ dimers in the gas phase, with a pronounced well (1.65 kJ mol^{-1}) for the fundamental singlet state where the molecules are separated by 3.56 \AA [21]. The same geometry was observed with high resolution electronic spectroscopy of $(\text{O}_2\text{-O}_2)$ dimers in a solid neon host at 4 K, with a distance between the molecules of 3.41 \AA [22]. Since the separation between neighboring molecules

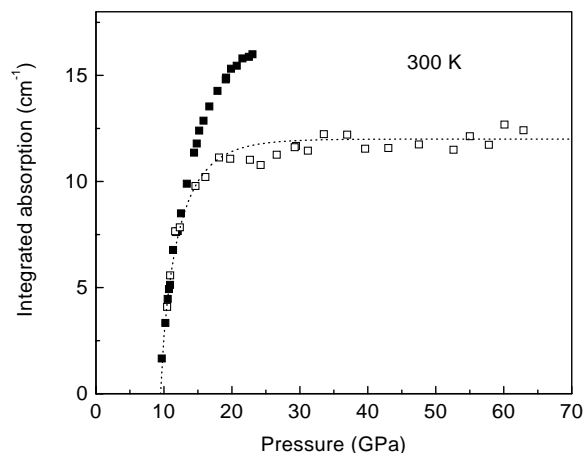


FIG. 3. Pressure behavior of the integrated absorption of the ν_{FIR} (open squares) and ν_{MIR} (solid squares) modes. The dashed line is a guide for the eye.

in the bc plane of the ϵ phase is 30% lower than these equilibrium distances, the picture of a new O₂-O₂ bond is therefore reasonable.

In the framework of an O₄ unit, six vibrational modes are expected: a symmetric (a_g) and an antisymmetric (b_{3u}) stretching mode involving the internal O-O bond, two analogous symmetric (a_g) and antisymmetric (b_{2u}) stretching motions involving the new O₂-O₂ bonds, and one in-plane (b_{1g}) and one out-of-plane (a_u) bending modes. A calculation performed on an O₂-O₂ dimer using density functional theory (B3LYP functionals) with the 6-31G(D) basis set (GAUSSIAN REV E.2) [23], provided frequency values of 204 and 1465 cm⁻¹ for the b_{2u} and b_{3u} antisymmetric stretching modes, respectively, and 1634 cm⁻¹ for the symmetric (a_g) stretching. These results furnish a qualitative guide to interpret our spectra. The antisymmetric libration b_{2u} of the two O₂ interacting molecules, which acts in the new unit as an antisymmetric intermolecular O-O stretching, is expected in a very low frequency region and it is assigned to the ν_{FIR} peak. The ν_{MIR} band is assigned to the b_{3u} O₄ vibration. The two antisymmetric stretching modes are infrared active in the isolated molecule, so that large infrared activity is expected in the crystal, as it is indeed observed. Therefore, the infrared (ν_{MIR}) and the Raman bands, observed, respectively, at about 1500 and 1600 cm⁻¹, are not relative to the Davydov components of the O₂ stretching mode but are originated by two different modes of the isolated O₄ molecule: the antisymmetric (b_{3u}) and the symmetric (a_g) vibrations. This interpretation is also supported by the gap between the densities of states (DOS) of these modes extracted by the analysis of the overtone region [24]. Also, the ν_{L2} (≈ 400 cm⁻¹) and ν_{L1} (≈ 200 cm⁻¹) bands observed in the Raman spectrum [20] are now easily assigned to the in-plane bending (b_{1g}) and to the symmetric intermolecular stretching (a_g) modes. Finally, the rapid frequency growth up to 20 GPa of the ν_{FIR} mode and the opposite behavior of the ν_{MIR} band is now understood on the basis of a charge density transfer which determines the formation of the new bond weakening the other. The dynamics of this process is clearly illustrated by the absorption versus pressure profile (see Fig. 3).

In conclusion, this analysis demonstrates that the oxygen metallization is anticipated by an association between molecules. In analogy with the data of Ref. [21], this state of the O₄ unit is predicted to be a singlet state. For this reason, it is expected that the ϵ phase of solid oxygen is nonmagnetic. These data also shed new light on the *ab initio* results of Serra *et al.* [25], where the nonmagnetic phase found in the calculation should be better identified with the nonmetallic ϵ than with the metallic ζ phase. For oxygen, a precise structural determination would greatly help to verify the result of this work.

We are grateful to Professor P.R. Salvi for helping us in the calculations and Professor M. Nicol for useful

discussions and suggestions. This work was supported by the European Union under Contract No. ERB FMGE CT 950017.

*Electronic address: gorelli@lens.unifi.it

†Electronic address: ulivi@ieq.fi.cnr.it

‡Electronic address: santoro@lens.unifi.it

§Electronic address: bini@chim.unifi.it

- [1] K. Takemura, S. Minomura, O. Shimomura, and Y. Fujii, *Phys. Rev. Lett.* **45**, 1881 (1980).
- [2] H. K. Mao and R. J. Hemley, *Science* **244**, 1462 (1989).
- [3] K. Shimizu, K. Suhara, M. Ikumo, M. I. Erements, and K. Amaya, *Nature (London)* **393**, 767 (1998).
- [4] M. Sakashita, H. Yamawaki, and K. Aoki, *J. Phys. Chem.* **100**, 9943 (1996).
- [5] C. S. Yoo and M. Nicol, *J. Phys. Chem.* **90**, 6732 (1986).
- [6] A. I. Katz, D. Schiferl, and R. Mills, *J. Phys. Chem.* **88**, 3176 (1984).
- [7] A. P. Ginsberg and J. L. Lundberg, *Inorg. Chem.* **10**, 2079 (1971).
- [8] S. Desgreniers, Y. K. Vhora, and A. L. Ruoff, *J. Phys. Chem.* **94**, 1117 (1990).
- [9] M. Nicol and K. Syassen, *Phys. Rev. B* **28**, 1201 (1983).
- [10] R. J. Meier and R. B. Helmholtz, *Phys. Rev. B* **29**, 1387 (1984).
- [11] F. A. Gorelli, L. Ulivi, M. Santoro, and R. Bini, *Phys. Rev. B* **60**, 6179 (1999).
- [12] S. W. Johnson, M. Nicol, and D. Schiferl, *J. Appl. Crystallogr.* **26**, 320 (1993).
- [13] S. Desgreniers and K. E. Brister, in: *High Pressure Science and Technology*, edited by W. A. Trzeciakowski (World Scientific, Singapore, 1996), p.363.
- [14] Y. Akahama, H. Kawamura, D. Hausermann, M. Hanfland, and O. Shimomura, *Phys. Rev. Lett.* **74**, 4690 (1995).
- [15] M. Nicol, K. R. Hirsch, and W. B. Holzapfel, *Chem. Phys. Lett.* **68**, 49 (1979).
- [16] S. F. Agnew, B. I. Swanson, and L. H. Jones, *J. Chem. Phys.* **86**, 5239 (1987).
- [17] R. Bini, R. Ballerini, G. Pratesi, and H. J. Jodl, *Rev. Sci. Instrum.* **68**, 3154 (1997).
- [18] R. Bini, L. Ulivi, J. Kreutz, and H. J. Jodl, *J. Chem. Phys.* (to be published).
- [19] H. Yamada and W. B. Person, *J. Chem. Phys.* **41**, 2478 (1964).
- [20] Y. Akahama and H. Kawamura, *Phys. Rev. B* **54**, 15602 (1996).
- [21] V. Aquilanti, D. Ascenzi, M. Bartolomei, D. Cappelletti, S. Cavalli, M. de Castro Víttores, and F. Pirani, *Phys. Rev. Lett.* **82**, 69 (1999).
- [22] J. G. Goodman and L. E. Brus, *J. Chem. Phys.* **67**, 4398 (1977).
- [23] M. J. Frisch *et al.* Gaussian, Inc., Pittsburgh, PA, 1995.
- [24] F. Gorelli, M. Santoro, L. Ulivi, and R. Bini, *Physica (Amsterdam)* **265B**, 49 (1999).
- [25] S. Serra, G. Chiarotti, S. Scandolo, and E. Tosatti, *Phys. Rev. Lett.* **80**, 5160 (1998).